

Secure and secret cooperation of robotic swarms by using Merkle trees

Eduardo Castelló Ferrer^{*1}, Thomas Hardjono², Marco Dorigo³, Alex ‘Sandy’ Pentland^{1,2}

¹MIT Media Lab, Massachusetts Institute of Technology, Cambridge, MA 02139, USA

²MIT Connection Science & Engineering, Massachusetts Institute of Technology, Cambridge, MA 02139, USA

³IRIDIA, Université Libre de Bruxelles, Brussels, Belgium

Email: {ecstll, hardjono, pentland}@mit.edu, mdorigo@ulb.ac.be

Abstract—Swarm robotics systems are becoming an important component of both academic research and real-world applications. However, in order to reach widespread adoption, new models that ensure the secure cooperation of these systems need to be developed. This work proposes a novel model to encapsulate cooperative robotic missions in Merkle trees. With the proposed model, swarm operators can provide the “blueprint” of the swarm’s mission without disclosing its raw data. In other words, data verification can be separated from data itself. We propose a system where robots in the swarm have to “prove” their integrity to their peers by exchanging cryptographic proofs. This work analyzes and tests the proposed approach for two different robotic missions: foraging (where robots modify the environment) and maze formation (where robots become part of the environment). In both missions, robots were able to cooperate and carry out sequential operations in the correct order without having explicit knowledge about the mission’s high-level goals or objectives. The performance, communication costs, and information diversity requirements for the proposed approach are analyzed. Finally, conclusions are drawn and future work directions are suggested.

Keywords—*Distributed Robotics; Cooperative Robotics; Data Privacy; Research Challenges; Merkle Trees; Verifiable Robotics; Trustable Robotics; Reliable Robotics*

I. INTRODUCTION

Swarm robotics systems [1] have the potential to revolutionize many industries, from targeted material delivery [2] to precision farming [3], [4]. Boosted by technical breakthroughs, such as cloud computing [5], [6], novel hardware design [7], [8], [9], and manufacturing techniques [10], swarms of robots are envisioned to play an important role in both industrial [11] and urban [12], [13] activities. The emergence of robot swarms has been acknowledged as one of the ten robotics grand challenges for the next 5-10 years that will have significant socioeconomic impact [14]. However, despite having such a promising future, many important aspects which need to be considered in realistic deployments are either underexplored or neglected [14].

One of the main reasons why swarms of robots have not been widely adopted in real-world applications is because there is no consensus on how to design swarm robotics systems that include perception, action, and communication among large groups of robots [14]. In addition, recent research points out that the lack of security standards in the field is also hindering the adoption of this technology in data-sensitive areas (e.g., military, surveillance, monitoring) [15]. These research gaps are motivating scientists to focus on new fields of study such as applied swarm security [16], [17] and privacy [18], [19] as well as to revisit already accepted assumptions in the field.

From the origins of swarm robotics research, robot swarms were assumed to be fault-tolerant by design, due to the large number of robot units involved [20], [21], [22], [23]. However, it has been shown that a small number of partially failed robots (with defective sensors, broken actuators, noisy communications devices, etc.) can have a significant impact on the overall system reliability and performance [24]. The first surveys on swarm robotics security were presented in [25], [26]. These works identified physical capture and tampering with members as significant threats to robot swarms. Physical capture of a robot might not only lead to loss of availability but also to the capture of security credentials or critical details of the swarm operation [27]. For instance, if a robot is tampered with and reintroduced into the swarm, an attacker might influence the behaviour of the whole system [23] and eventually hinder the entire operation [28]. These attacks would be unique to swarm robotics technology and are particularly critical in situations where robot swarms must share data among individual robot units or with human operators.

In previous swarm robotics work, researchers hard-coded the complete set of rules that trigger the transitions from task to task [22], [29], [30] in all the robots within a mission. Although this distributed approach is more robust and fault-tolerant than centralized methods, it significantly increases the attack surface (i.e., total sum of vulnerabilities) for an attacker to figure out the swarm’s high-level goals and modify the system’s behavior [27]. Due to these concerns, in this work, we aim to shed light on the following questions: How can we make sure that robot swarms can cooperate while minimizing security risks such as physical capture or tampered members? Is there a way to provide the “blueprint” of a robotic mission without describing the mission itself? In other words, is it possible that robot swarms fulfill step-by-step (i.e., sequential) missions without having explicit knowledge about the mission’s objectives? To answer these questions, we propose a model which allows robots to cooperate without exposing the high-level information about the swarm’s goals. To do so, we explore for the first time the idea of encapsulating robotic missions into Merkle trees. More specifically, we introduce a framework where data verification is separated from data itself. By exchanging cryptographic “proofs” within the swarm, robots are able to “prove” to their peers that they know specific pieces of information included in the swarm’s mission and therefore cooperate towards its completion.

The remainder of this paper is structured as follows. Section II summarizes related work on Merkle trees and their applications outside the robotics field. Section II-A provides a formalization of Merkle trees and introduces the concept of “proof”. Section III describes the setup of our experiments including the type of mission, robots, simulator and analysis

^{*}Corresponding author: Eduardo Castelló Ferrer, ecstll@mit.edu

metrics used to evaluate the proposed approach. Section IV presents the results of our experiments. Section V discusses the results obtained and proposes future directions where our approach also shows promising results. Finally, Section VI provides our conclusions.

II. MERKLE TREES

A Merkle Tree (MT) [31] is a hash-based tree structure where data is not stored in the interior nodes but in the leaves. MTs belong to the family of Authenticated Data Structures (ADS), a type of data objects whose operations can be carried out by an untrusted third party. Two main roles, *provers* (P) and *verifiers* (V), are involved when using MTs. Provers store the data of interest encapsulated in an MT and are able to answer queries about it. Verifiers send queries to provers and in exchange they receive a “proof”. A proof is a piece of information by which one party (P) can demonstrate to another party (V) that they know a value, without conveying any information apart from the fact that they know that specific value. Verifiers can check whether any piece of information belongs to the MT by checking the validity of the proof received. Fig. 1 shows a general description of this process. MTs have two main properties: correctness and security. On the one hand, correctness implies that a proof can be easily generated to verify and demonstrate that a piece of information is known and correct. This can be done without exposing the raw information itself by using cryptographic hashes. On the other hand, security implies that a computationally bounded, malicious agent cannot forge an incorrect result and therefore only agents that know the appropriate information can generate valid proofs.

In previous literature, MTs have been used in a wide variety of applications ranging from efficient data authentication [32], sharing [33] and integrity [34], to validation in large datasets, sensor networks [35], [36], software updates [37], etc. However, to the best of our knowledge, no research work has focused on the use of MTs in the field of robotics. In this work, we propose a model by which high-level missions can be encapsulated within an MT as a set of atomic operations performed by a swarm of robots. By searching the environment, robots are able to obtain sensor information and check whether potential actions are included in the MT (or not). In

the affirmative case, robots are able to use MT proofs to prove to their peers that certain parts of the mission were discovered, carried out, and completed.

A. Merkle tree proofs

An MT of depth d is a tree with $n = 2^{d-1}$ leaf nodes: x_0, \dots, x_{n-1} , where each leaf node encapsulates a hash string of an associated operation, while each interior node contains the hash of the combination of its two children. A depiction of a complete MT for $d = 3$ is given in Fig. 2(a). Each leaf node (green blocks) encapsulates the combined hash of two hashes: h_s (sensor’s input) and h_a (robot’s action). These two hashes describe an atomic operation within the swarm’s high-level mission. For instance, the hash of the action “carry to target” (h_a) and the hash of the sensor input “red token” (h_s) would be included in one of the leaf nodes by using the hashing function $H: H_{x_i} = H(h_a, h_s)$. As outlined in Fig. 1, when V queries P it retrieves the value x_i at index $i \in [0, n - 1]$. Then, P returns the value x_i together with a chain of digests π needed to compute the root node digest (red block). V keeps (at least) a copy of the root node hash itself, and checks π by trying to recompute the root node hash in a bottom-up manner.

Fig. 2(b) shows the proof π for a fetch at the leaf position x_1 . It consists of four elements in sequence, the two hashes h_a and h_s , the hash H4, and the hash H3. Then, the verification proceeds bottom up: V computes the hash of the two hashes h_s and h_a , which is H5, and concatenates it with the hash of H4 provided in π . Next, it concatenates H4 and H5 and computes the hash of what should be the digest for node H2. Then, it concatenates H3 provided in π , with its computed digest from the previous process, and hashes the result. Finally, it confirms whether this computed digest equals H1 (root node hash).

As mentioned before, we are interested in MT’s correctness and security. First, correctness implies that when P executes a query Q over its own MT, then V gets the same outcome as it would have if it had just computed Q locally. This property opens the path to secret cooperation between agents since encrypted verification data can be exchanged within the swarm without disclosing any “raw” or “unprotected” information. Second, security implies that a computationally limited, deceiving P cannot induce V to admit a faulty answer. The basis of this property is the use of collision-resistant hashes: if P can cause V to accept an incorrect answer then the proof returned by P will yield a collision (i.e., two different inputs produce the same output hash value). This research assumes the hash generation method used (SHA3-256) is collision-free, since the probability that different inputs produce the same output is negligible. This property leads the way to secure cooperation between agents.

III. EXPERIMENTAL SETUP

Fig. 3 shows the initialization process of our experiments. We assume that an external entity (e.g., the swarm’s operator) designed and pre-computed a valid MT where all operations to fulfill the swarm’s mission are included in the correct order (1). Then, the resultant MT is broadcast to all the robots (2) before the mission starts (3). During the mission, robots can check whether the combined hash of potential actions (h_a) upon specific sensor’s inputs (h_s) can be related to their MT copy by trying to generate a valid proof. In this work, we tackle the case in which m operations must be

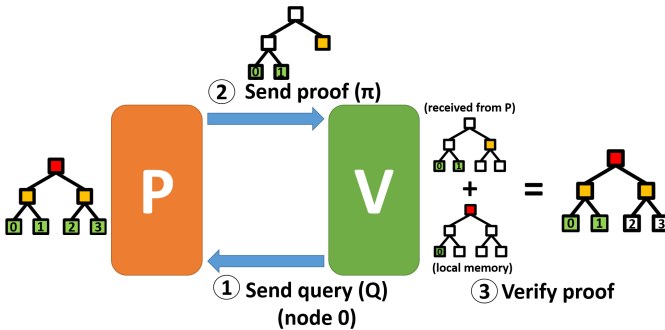
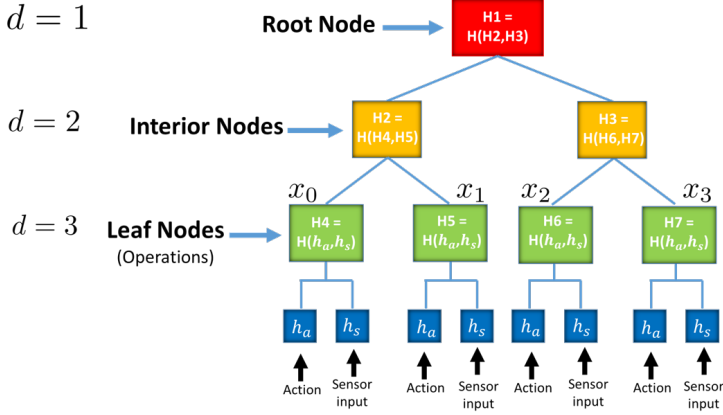


Figure 1. Workflow between *provers* (P) and *verifiers* (V). (1) V sends a query (Q) to P regarding a particular node (e.g., node 0). (2) P sends a proof π (chain of hashes) that demonstrates knowledge about the requested node. (3) V verifies the proof by computing in a bottom-up fashion the received information. The proof is regarded as valid if V can generate the root node it kept in memory by using π .

(a)



(b)

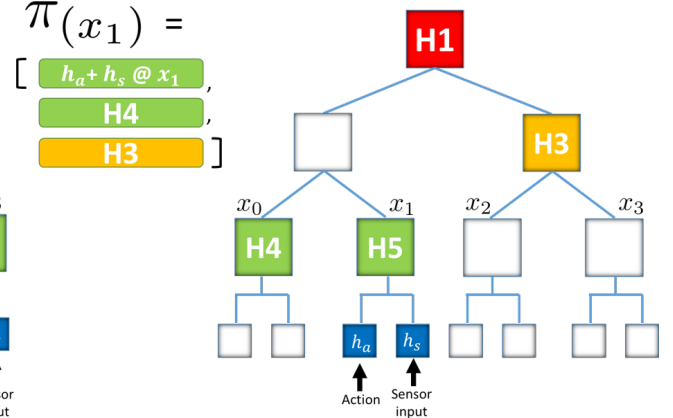


Figure 2. (a) Merkle Tree (MT) implementation ($d = 3$) with 4 leaves, 2 interior, and 1 root nodes. Each leaf node (green) encapsulates the hash of two hashes: a robot action (h_a) and a robot sensor input (h_s). Each leaf node represents one atomic operation robots should complete sequentially (x_0, x_1, \dots, x_{n-1}) in order to fulfill the swarm's mission. Interior nodes encapsulate the hash of their two children, the same way that the root node encapsulates the hashes of its two interior nodes. (b) Describes the path (in color) in order to get the proof for leaf node x_1 .

performed in a specific order (i.e., sequentially) and without repetitions. As described in [38], our problem scenario can be understood as a single operation (SO), single robot (SR), and instantaneous Assignment (IA) scenario: SO-SR-IA. In SO, robots are only able to execute one operation at a time. In SR, operations requires exactly one robot to achieve them. Finally, IA means that the available information concerning the robots, the operations, and the environment permits only an instantaneous allocation of operations to robots, with no planning for future allocations. The mission is finished once all operations are fulfilled in the right order and the MT is therefore regarded as completed.

A. Foraging mission

We consider a robot foraging mission where a sequence of colored tokens have to be delivered to a target location. Each operation in this mission implies searching, retrieving, and transporting one token to the center of the arena. After the token is deposited in the target, robots can regard that operation as completed and therefore exchange its corresponding MT proof. The foraging mission is considered completed when at least one robot (i.e., the carrier of the last token) completes its entire MT. It is important to note that the order in which these colored tokens have to be delivered is *a priori* unknown to the robots, since they only count with the hash values included in

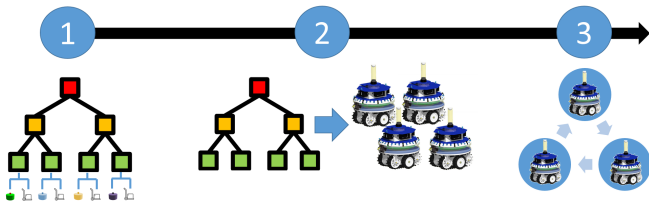


Figure 3. Experiment's initialization process. (1) The swarm's operator generates a valid MT where all the operations that fulfill the swarm's mission are included in the correct order. (2) The MT is broadcast to all robots in the swarm. (3) The experiment starts.

the MT.

Fig. 4 is a snapshot of the simulation arena where the foraging experiments were conducted. The environment consists of a rectangular area ($5 \times 5 \text{ m}^2$) with a central black square ($0.5 \times 0.5 \text{ m}^2$) representing the target location where foot-bot robots [29] (Fig. 5(a)) need to transport the correct sequence of discovered tokens. Fig. 5(b) depicts one of the solid green cylinders that is used as a token within the experiments. These tokens are 5 cm tall and 10 cm in diameter and have a LED marker at the top that defines the token color. Tokens of different colors represent different sensor inputs. In this work, the color k of a token is chosen in the set $\{\text{green, red, blue, yellow, magenta, cyan, white, orange}\}$. A certain number D_k of tokens of each color k were randomly positioned in the arena at the beginning of each simulation run. All the experiments were conducted in ARGoS [39], a modular multi-robot simulator and development environment.

Fig. 6 depicts the finite state machine (FSM) that controls the robot for the foraging mission, which relies on three basic behaviors:

Wander. The robot performs a random walk searching for

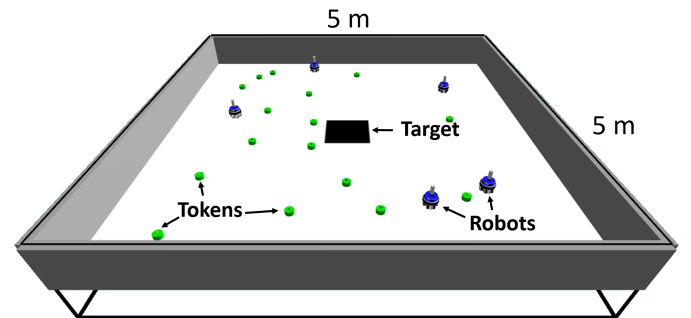


Figure 4. Simulation arena used in the foraging mission. The scenario consists of a rectangular area of $5 \times 5 \text{ m}^2$ that provides adequate space for a small swarm of robots within which robots, tokens, and a target location are placed.

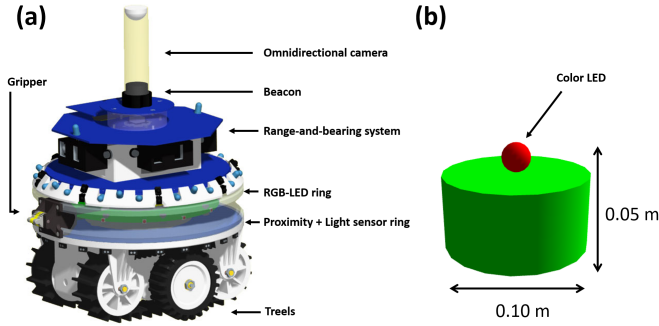


Figure 5. (a) Diagram of the simulated foot-bot together with its sensors layout. Foot-bot’s size and features correlate with real-world models for swarm and multi-agent systems. (b) Token used in the experiments. Tokens simulate 3D printed cylinders with the following dimensions: 5 cm tall and 10 cm in diameter. The colored sphere at the top of the token represents an LED marker to visually track and identify the tokens.

tokens. If the robot detects a token within its vision range ($\text{Token.distance} \leq V_{range}$), it executes the **Check** behavior; otherwise it continues searching. During the execution of this action the robot is able to detect obstacles such as walls or other robots (within distance O_{range}) and avoid them.

Check. Once a token is within the robot’s vision range, the robot can extract sensor information (point cloud data, RFID data, etc.) from it. In this stage, robots perceive the color of the LED marker associated with each of the tokens as a sensor input. This information is used by the robots in order to generate the sensor input hash (h_s). For the considered foraging task, the action hash h_a encodes the “carry to target” action. Robots executing the **Check** behavior combine h_s and h_a to generate a meta-hash ($H_{x_i} = H(h_s, h_a)$) that is used to generate the proof π . In case a proof π exists for the current working leaf node x_i : $\exists \pi(x_i, H_{x_i})$, the combination of token color and action (i.e., operation) can be verified as part of the MT. Otherwise ($\exists! \pi(x_i, H_{x_i})$), the robot returns to the **Wander** behavior.

Handle. In case the robot generates a valid proof for the visible token, the robot approaches the token until it reaches a grabbing distance. In that moment, the robot activates its

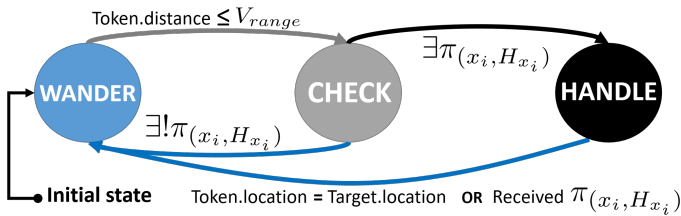


Figure 6. Finite state machine for the robot behavior. Three behaviors—**Wander**, **Check**, and **Handle**—are coded in every robot. Robots executing the **Wander** behavior search the environment looking for tokens. Once a token is found, robots execute the **Check** behavior. Then, robots extract the information from the token (i.e., its color) and generate both h_s and h_a . H_{x_i} is calculated from rehashing h_s and h_a : $H_{x_i} = H(h_s, h_a)$. H_{x_i} is verified against the current working leaf node (x_i) of the robot’s MT. In case it is possible to generate a valid proof with the token’s information ($\exists \pi(x_i, H_{x_i})$), the robot executes the **Handle** behavior: this makes the robot grab the token and place it in the target location (arena center). If not, the robot returns to the **Wander** behavior. Robots stop executing the **Handle** behavior once the token is placed in the target location or they receive the proof that x_i was already completed.

gripper (Fig. 5(a)), grabs the token, and transports it to the center of the arena. Once the robot reaches its destination ($\text{Token.location} = \text{Target.location}$), the robot releases the token and changes the status of the x_i node as completed in its local MT. Then, the robot increments the pointer of the current working leaf node: $x_i = x_i + 1$ for $x_i \in (0 \leq x_i \leq n - 1)$. In case the robot receives a proof that the x_i has been already completed by another robot while carrying the token, the robot drops the token and returns to the **Wander** behavior.

Fig. 7, shows the robot interaction space. It is important to note that during the execution of the three behaviors explained previously, robots can exchange information with their peers (e.g., x_i, π). If robots are within a C_{range} distance from other robots, these can compare their MT copies by sending queries (Q) about their correspondent working leaf nodes (x_i) and receive proofs (π) in exchange as depicted in Fig. 1. By using this method robots can update, synchronize, and complete their own MT copies and therefore cooperate towards the fulfillment of the swarm’s mission.

B. Maze formation mission

In the maze formation mission, instead of having the robots modify the environment (e.g., transport tokens), we let them become part of the environment.

Fig. 8(a) represents the “blueprint” of a 5×5 maze where 0 represents an empty space, 1 a wall, and * and @ the entrance and the exit of the maze, respectively. As illustrated in Fig. 3, we generated (at design time) a complete MT where leaf nodes encapsulate maze coordinates (instead of token colors). According to their FSM controller (Fig. 6), robots start exploring the arena executing the **Wander** behavior. Robots are able to locate themselves (Fig. 7) in the 2D arena ($5 \times 5 \text{ m}^2$). By knowing the cell dimensions ($1 \times 1 \text{ m}^2$) they can calculate the (x,y) coordinates of the grid depicted in Fig. 8(a). Every time a robot enters a new cell it executes the **Check** behavior. Then, robots use the current grid (x,y) components to calculate

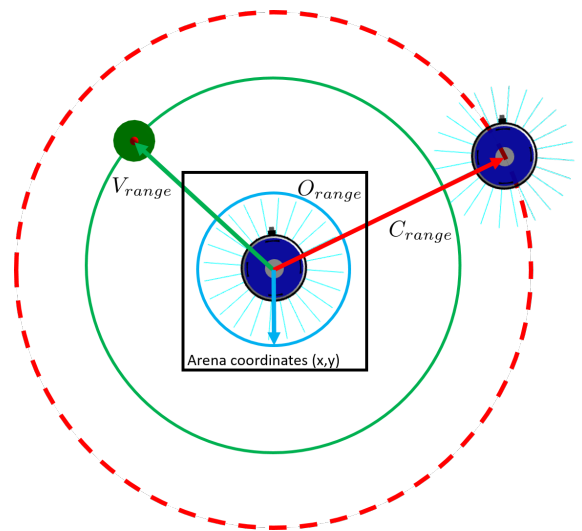


Figure 7. Robot communication and interaction diagram. Every robot controller relies on three main thresholds: O_{range} represents the range where obstacles are detected by robots in order to avoid collisions. V_{range} represents the robot’s maximum vision range to detect tokens. C_{range} represents the minimum required distance for robots to communicate with one another.

the h_s digest and the hash of the action “stop” as h_a . In case robots generate a valid proof π , they execute the **Handle** behavior, which leads them to find the center of the cell and stop there (Fig. 8(b)). In the same way as in the foraging mission, robots avoid already completed operations (in this case stop in already occupied cells) by receiving the proof that their current working leaf node (x_i) was already completed. In contrast to the foraging example, the maze formation mission is finished once all operations have been completed as well as all the robots have completed their MTs.

C. Analysis metrics

In order to evaluate and analyze the proposed approach we rely on three metrics:

Performance. Performance measures how fast and reliably a particular mission is carried out. In this paper, we use the mission’s finishing time F_t to measure the amount of time required to fulfill the swarm’s mission. In addition, we use an estimate P_s of the probability that the system attains its target objective in an amount of time τ [40]. Formally, let $j \in \{1, \dots, k\}$ be the index of an experiment, r_j be the run time of experiment j , and experiments that fulfill $r_j < TC$ (Time Cap) be successful experiments. The estimate \hat{P}_s of the probability of success of the system over time (up to TC) is defined as $P_s(\tau \leq t) = \{j | r_j \leq t\} / k$.

Communication cost. To measure communication costs, we use the Communication Cost (CC) metric. CC represents the number of times the P-V workflow (Fig. 1) takes place during the mission multiplied by the size (in bytes) of the proof (π) the robots exchanged. When the MT is perfectly balanced ($n = 2^{d-1}$), the size of the proof π is $\log_2(n) + 2$: the number of hashes to reach the root node plus the h_s, h_a hashes. In missions where all robots need to complete their MTs — as for example in the maze formation mission — CC can be accurately calculated with the following equation:

$$CC = P_n \cdot P_l \cdot |H| \quad (1)$$

where $P_n = ((R_n - 1) \cdot n)$ is the total number of proofs exchanged, $P_l = \log_2(n) + 2$ is the length of the proof, and $|H|$ is the size (in bytes) of the hash function used. The hash

function used in this work (SHA3-256) has a hash size ($|H|$) of 32 bytes.

Information diversity. In this research, robots are only in contact with the raw sensor and action information from the operations they carry out themselves. However, in swarm robotics applications, it is difficult to fully ensure robots fulfill only one operation per mission. Therefore, certain robot units might be able to accumulate raw or unprotected information that could be stolen if they are subject to attacks (e.g., physical capture). To analyze this phenomenon, we introduce Shannon’s equitability (I_e) to measure “evenness”, that is, to measure how widely spread raw information is within the swarm.

Shannon’s equitability (I_e) can be calculated by dividing Shannon’s index I by I_{max} :

$$I_e = \frac{I}{I_{max}} \quad (2)$$

where Shannon’s index $I = -\sum_{i=1}^S p_i \ln p_i$ (i.e., Shannon’s entropy [41]) is a mathematical measurement used to characterize diversity (S is the total number of operations in the mission and p_i is the proportion of S made up of the i^{th} operation), and where $I_{max} = \ln S$.

I_e assumes a value between 0 and 1, with 1 being complete “evenness”: all robots carried out the same number of operations and therefore were exposed to the same amount of raw information.

IV. RESULTS

A set of 50 simulation experiments were carried out to analyze the proposed approach in the foraging scenario shown in Fig. 4. MTs with different n values were used in order to increase the complexity and duration of the swarm’s foraging mission. In addition, the following parameters were used: $D_k = 4$, which implies that in simulations where the MT has 4 leaf nodes ($n = 4$), a total of 16 tokens are present in the simulation arena. Experiments were run using R_n robots, $R_n \in \{1, \dots, 5\}$. The robot communication range (C_{range}) was initialized to 2 m, the vision sensing distance (V_{range}) was fixed to 0.50 m, and finally the robot obstacle detection range (O_{range}) was initialized to 0.10 m. The Time Cap (TC) for each experiment was set to 10,000 seconds.

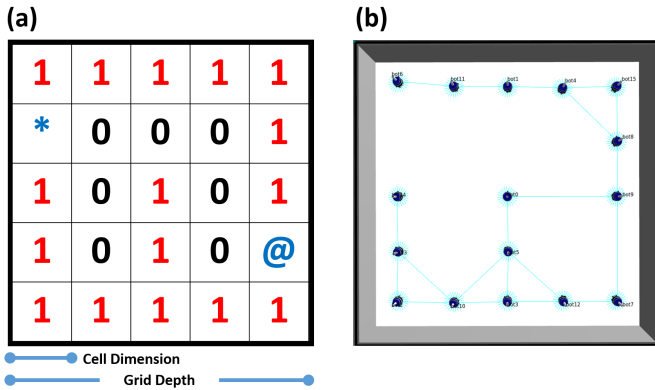


Figure 8. (a) 5x5 matrix used in order to represent a maze. Four different elements are included in the array: 0 (black) represents an empty space, 1 (red) represents a wall, * and @ (blue) represent the entrance and the exit of the maze, respectively. (b) The maze depicted in (a) built by a swarm of robots using the approach presented in this paper.

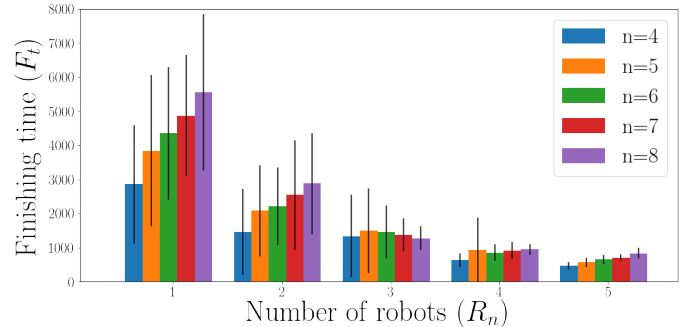


Figure 9. Average F_t (in secs) and standard deviations for different MT lengths (n) and robot swarm sizes (R_n). Averaged results for the execution of an MT with 4 (blue), 5 (ochre), 6 (green), 7 (red), and 8 (purple) leaf nodes.

Fig. 9 shows the finishing times (F_t) and standard deviations for several MT length configurations (n) and robot swarm sizes (R_n). According to Fig. 9, the addition of more

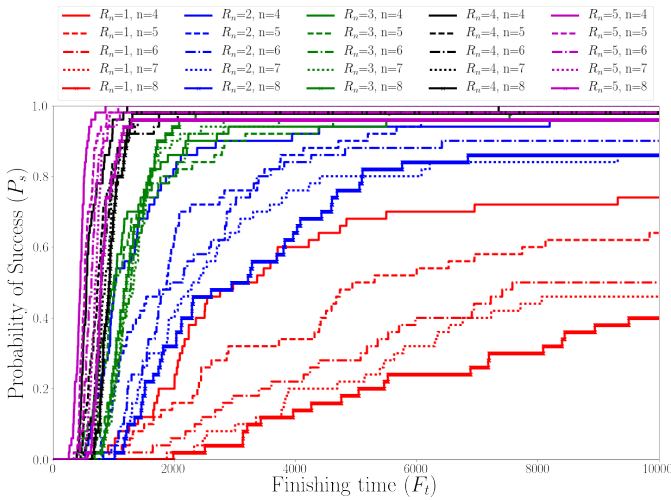


Figure 10. Probability of success (P_s) for each one of the different configurations shown in Fig. 9. Empirical run-time distributions for the execution of the foraging task with $R_n = 1$ (red), 2 (blue), 3 (green), 4 (black), and 5 (purple). For each one of these configurations solid ($n = 4$), dashed ($n = 5$), dot-dashed ($n = 6$), dotted ($n = 7$), and asterisk-solid ($n = 8$) lines were included.

robots decreases the F_t of the foraging mission regardless of the length of the MT. However, these results suggest that once a certain number of robots is present ($R_n \geq 3$), the length of the MT has a small impact on the F_t of the system. Fig. 10 shows the progression of P_s for all the configurations presented in Fig. 9. According to Fig. 10, the addition of more robots increases P_s since lines become steeper and converge to higher values sooner. However, these results also suggest that as we increase n (the mission becomes longer), P_s converges to lower values or reaches higher values later (especially for $R_n \leq 3$). It is important to note that P_s does not reach 1 (the maximum value) in several configuration as experiments were run up to TC and before convergence.

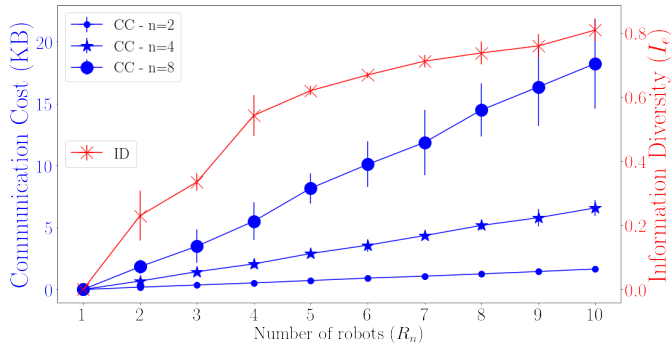


Figure 11. Communication Cost (CC) and information diversity (I_e) metrics in blue and red colors, respectively, for different R_n and n values. Averaged results and standard deviations suggest a direct relationship between the two metrics in the foraging mission.

Fig. 11 shows averaged results and standard deviations for the communication cost (CC) in KB and information diversity measured by Shannon's equitability index (I_e) for different R_n ($1 \leq R_n \leq 10$) and $n \in \{2, 4, 8\}$ configurations. Fig. 11 shows that CC increases linearly with R_n since there are more robots exchanging information. Moreover, MTs with larger n values also seem to increase the CC since the proofs robots

exchange are "heavier". Larger standard deviation values, as R_n increases, imply that there is no fixed number of P-V workflows required to make one robot complete its MT (finishing condition of the foraging mission). However, larger R_n values tend to increase the information diversity (I_e) in the swarm. This result suggests that, as we increase R_n , the information in the swarm tends to become more diversified. Fig. 11 also suggests that information diversity might have an asymptotic behavior around 0.8 and a really large R_n value might be necessary to converge to 1 (i.e., to complete "evenness").

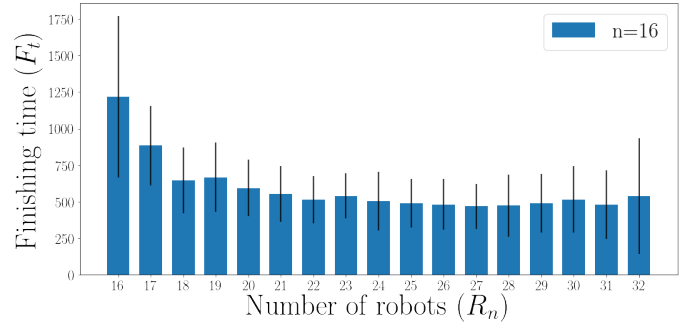


Figure 12. Average F_t (in seconds) and standard deviations for the maze formation mission with different robot swarm sizes. All results were obtained with a maze of an MT with 16 (blue) leaf nodes ($n = 16$).

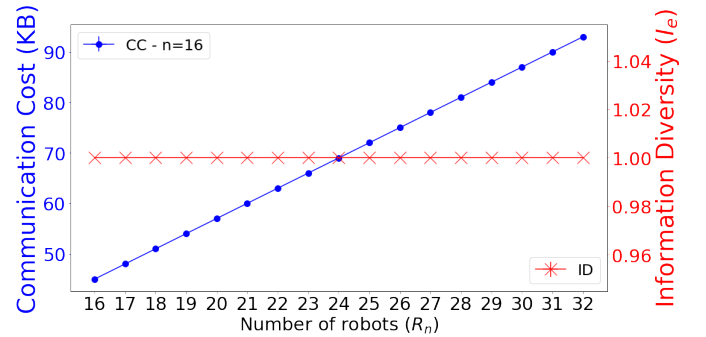


Figure 13. Communication cost (CC) and information diversity (I_e) metrics in blue and red colors, respectively, for different R_n values for the maze formation mission. Average results suggest no direct relationship between the two metrics.

To complement the results introduced previously, an additional set of 25 simulation experiments was carried out to analyze the maze formation mission (Fig. 8). In this case, n was fixed to 16 in order to match the number of cells where the value 1 is present in Fig. 8(a). In addition, R_n ($n \leq R_n \leq 2n$). Fig. 12 shows average F_t and standard deviations for the maze formation mission. Fig. 12 shows the same behavior as its foraging counterpart (Fig. 9): larger R_n values reduce F_t . However, beyond a certain R_n value ($R_n \geq 20$), no real impact on F_t can be seen. Complementarily, Fig. 13 shows the CC and I_e metrics for the maze formation mission. This figure also shows that CC increases linearly with R_n . However, in contrast to Fig. 11, the absence of standard deviations confirms that a fixed CC is required to make all robots complete their MTs (finishing condition of the maze formation mission). Finally, Fig. 13 depicts a scenario where complete "evenness" of information (i.e., $I_e = 1$) is achieved. This is possible since in the maze formation mission, when

robots find a cell where they can generate a valid π proof, they stop at its center, thereby, making robots capable of fulfilling only one operation per mission, in contrast to the foraging scenario, where one robot might be able to complete several operations.

V. DISCUSSION

In this research, we show how two of the main MT properties (i.e., correctness and security) open a new path towards secure and secret cooperation in robot swarms. Regarding the security aspect, by using the proposed approach, robots in a swarm are required to “prove” to their peers that they fulfilled certain actions or that they know or “own” particular information (i.e., proof-of-ownership [42]) to cooperate, rather than merely rely on information received from other robots (sensor data, votes, etc.). This approach makes robots resistant against potential threats such as tampering attacks since any alternation in the operation’s data (e.g., h_s , h_a) will necessarily change the proof’s outcome. Regarding the secrecy component, with the use of MTs swarm robots are now able to separate the mission data from its verification. This allows robots to verify that an operation was carried out by a member of the swarm without knowing what this operation entailed or which robot took part in its completion. This makes physical capture attacks inefficient since individual robots might not have enough raw or unprotected information to describe the high-level swarm’s missions and goals, especially in large systems. However, this doesn’t prevent swarm robots from cooperating to fulfill complex missions since robots can still prove to their peers that certain operations were discovered, carried out, and completed.

The proposed approach was tested in two different scenarios: a foraging and a maze formation mission. In the foraging case, results suggest that R_n maintains an inverse relationship with F_t and a direct relationships with P_s . Therefore, increasing the swarm size has a positive impact on the performance of the system. However, results also show that CC grows linearly as the swarm size (R_n) increases, which in extreme situations (e.g., very large swarms) could represent a negative effect on the system since individual robots might not be able to cope with the bandwidth requirements. In contrast, increasing R_n has the positive effect of increasing I_e since we are increasing the probabilities of reaching more “even” distributions of completed operations within the swarm. In the maze formation mission, where R_n and n take larger values, results also suggest that R_n maintains an inverse relationship with F_t , I_e is maximized (i.e., $I_e = 1$), and even though CC grows linearly, this still does not represent a challenging situation for the swarm (e.g., 90 KB for a 32 robot system). It is interesting to emphasize that due to these properties, swarm robots can fulfill complex missions such as the maze formation one without the means to infer high-level details such as where the entrance or the exit might be located.

Encouraged by these results, we found appropriate to analyze the feasibility of the proposed approach in complex missions where the number of operations takes relatively large values. Fig. 14 shows different LEGO® models where a sequential set of operations is required to achieve the final outcome (i.e., build the replica). These models² are good projections of the missions presented in this work, especially

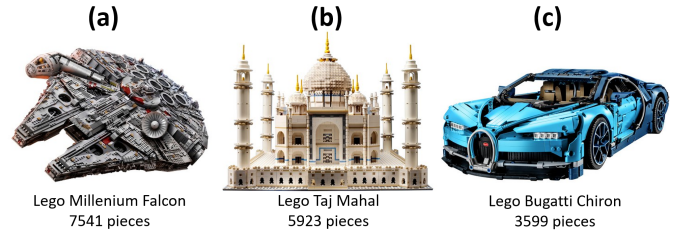


Figure 14. Different LEGO® models with their corresponding piece count. LEGO® models are a good example of complex sequential missions that could be encapsulated in Merkle trees.

Fig. 14	Memory (KB)	CC/R_n (MB)	ACT (s)
(a) Millennium Falcon (7541 pieces)	235 KB	3.39 MB	G: 8.45 (4.86) P: 0.0005 (1.54 e−5) V: 0.0006 (2.10 e−5)
(b) Taj Mahal (5923 pieces)	185 KB	2.54 MB	G: 6.62 (3.81) P: 0.0005 (1.87 e−5) V: 0.0006 (1.53 e−5)
(c) Bugatti Chiron (3599 pieces)	112 KB	1.46 MB	G: 4.01 (2.30) P: 0.0004 (1.58 e−5) V: 0.0005 (1.71 e−5)

TABLE I. Memory, Communication Cost per robot (CC/R_n), and Average Computation Time (ACT) requirements (with standard deviations in brackets) for the models depicted in Fig. 14. All ACTs were obtained by using the Raspberry Pi 3 Model B+ SBC.

since n takes a relatively large value. Due to the possibility of accurately calculating the amount of CC required to make all robots complete their MTs (Eq. 1) as well as the overall size of the MT stored by robots, we can compute Fig. 14’s corresponding MTs and measure their memory, communication cost per robot (CC/R_n) and Average Computation Time (ACT) requirements. For the latter, we included the following measures: generation of the complete Merkle tree (G), generation of a proof (P), and verification of a proof (V). Initial results for the aforementioned models are given in Table I.

Table I shows that neither the memory, nor the communication cost per robot, nor the average computation time of the corresponding MTs is out of reach of current commodity hardware (e.g., Raspberry Pi 3 Model B+) and therefore it is feasible for current robot platforms. It is important to note that more than 99% of the computation time is taken by the generation (G) of the MT that only takes place at the beginning of the mission, while the proof assembly (P) and validation (V) take an almost insignificant amount of time.

VI. CONCLUSIONS

Swarm robotics is starting to show potential in both academic and real-world scenarios. However, achieving secure behaviors for large numbers of robots is still a challenging problem. Recent studies have emphasized the importance and lack of solutions for the security and privacy issues in the distributed robotics field. Merkle trees are binary hash-tree structures with two main properties: correctness and security. These properties have the potential to achieve secure and secret robot cooperation and therefore make robot swarms resistant against tampered members and physical capture attacks. By using Merkle trees, swarm operators can provide the

²Three of the replicas with the largest piece count according to the current LEGO® catalog: <https://shop.lego.com/en-US/>

“blueprint” of the swarm’s objectives without disclosing raw or unprotected data about the mission itself. The performance, communication costs, and information diversity metrics of the proposed combination were analyzed for two different sequential missions: foraging (where robots modify the environment) and maze formation (where robots become the environment). Results show that larger numbers of robots tend to increase the performance of the system as well as diversify the amount of information within the swarm. However, an increasing number of robots as well as longer missions scale linearly together with the communication requirements of the system. Nevertheless, an initial analysis on the storage, communication costs, and computational time for higher-scale missions reveals that the use of Merkle trees for current robotic technology is within reach.

ACKNOWLEDGMENT

This project has received funding from the European Union’s Horizon 2020 research and innovation programme under the Marie Skłodowska-Curie grant agreement No. 751615. Marco Dorigo acknowledges support from the Belgian F.R.S.-FNRS, of which he is a Research Director.

REFERENCES

- [1] M. Dorigo, M. Birattari, and M. Brambilla, “Swarm robotics,” *Scholarpedia*, vol. 9, no. 1, 2014, p. 1463.
- [2] R. D’Andrea, “Guest editorial: A revolution in the warehouse: A retrospective on Kiva Systems and the grand challenges ahead,” *IEEE Transactions on Automation Science and Engineering*, vol. 9, no. 4, 2012, pp. 638–639.
- [3] T. Blender, T. Buchner, B. Fernandez, B. Pichlmaier, and C. Schlegel, “Managing a mobile agricultural robot swarm for a seeding task,” in *IECON 2016 - 42nd Annual Conference of the IEEE Industrial Electronics Society*, Oct 2016, pp. 6879–6886.
- [4] D. Albani, J. Jsselmuiden, R. Haken, and V. Trianni, “Monitoring and mapping with robot swarms for agricultural applications,” in *2017 14th IEEE International Conference on Advanced Video and Signal Based Surveillance (AVSS)*, Aug 2017, pp. 1–6.
- [5] Y. Chen, Z. Du, and M. García-Acosta, “Robot as a service in cloud computing,” in *Proceedings of the 2010 Fifth IEEE International Symposium on Service Oriented System Engineering*, ser. SOSE ’10. Washington, DC, USA: IEEE Computer Society, 2010, pp. 151–158. [Online]. Available: <http://dx.doi.org/10.1109/SOSE.2010.44>
- [6] H. He, S. Kamburugamuve, G. Fox, and W. Zhao, “Cloud based real-time multi-robot collision avoidance for swarm robotics,” vol. 9, 06 2016.
- [7] M. H. A. Majid and M. R. Arshad, “Design of an autonomous surface vehicle (asv) for swarming application,” in *2016 IEEE/OES Autonomous Underwater Vehicles (AUV)*, Nov 2016, pp. 230–235.
- [8] Y. Mulgaonkar, A. Makineni, L. Guerrero-Bonilla, and V. Kumar, “Robust aerial robot swarms without collision avoidance,” *IEEE Robotics and Automation Letters*, vol. 3, no. 1, Jan 2018, pp. 596–603.
- [9] D. Rus and M. T. Tolley, “Design, fabrication and control of origami robots,” *Nature Reviews Materials*, vol. 3, no. 6, 6 2018, pp. 101–112.
- [10] E. Castello Ferrer and S. Y. Hanay, “Demo: A low-cost, highly customizable robotic platform for testing mobile sensor networks,” in *Proceedings of the 16th ACM International Symposium on Mobile Ad Hoc Networking and Computing*, ser. MobiHoc ’15. New York, NY, USA: ACM, 2015, pp. 411–412. [Online]. Available: <http://doi.acm.org/10.1145/2746285.2764935>
- [11] D. Chaudhari and S. A. Bhosale, “A review on management of logistics using swarm robotics,” in *2016 International Conference on Communication and Signal Processing (ICCCSP)*. IEEE, apr 2016, pp. 0371–0373.
- [12] “Method and system for autonomous or semi-autonomous delivery,” U.S. Patent US20 180 232 839A1, April 9, 2018.
- [13] A. L. Alfeo et al., “Urban swarms: A new approach for autonomous waste management,” *CoRR*, vol. abs/1810.07910, 2018.
- [14] G.-Z. Yang et al., “The grand challenges of science robotics,” *Science Robotics*, vol. 3, no. 14, 2018.
- [15] P. Scharre, “Robotics on the Battlefield Part II: The Coming Swarm,” Center for New American Security, Tech. Rep., 10 2014.
- [16] R. N. Akram et al., “Security, Privacy and Safety Evaluation of Dynamic and Static Fleets of Drones,” 2017.
- [17] S. Gil, S. Kumar, M. Mazumder, D. Katabi, and D. Rus, “Guaranteeing spoof-resilient multi-robot networks,” *Autonomous Robots*, vol. 41, no. 6, Aug 2017, pp. 1383–1400.
- [18] A. Prorok and V. Kumar, “A macroscopic privacy model for heterogeneous robot swarms,” in *Lecture Notes in Computer Science (including subseries Lecture Notes in Artificial Intelligence and Lecture Notes in Bioinformatics)*, ser. Lecture Notes in Computer Science, M. Dorigo et al., Eds. Springer International Publishing, 2016, vol. 9882 LNCS, pp. 15–27.
- [19] A. Prorok and V. K., “Towards differentially private aggregation of heterogeneous robots,” in *Distributed Autonomous Robotic Systems: The 13th International Symposium*. Springer International Publishing, 2018, pp. 587–601.
- [20] A. L. Christensen, R. O’Grady, M. Birattari, and M. Dorigo, “Exogenous fault detection in a collective robotic task,” in *Advances in Artificial Life, Proceedings of ECAL 2007*, ser. Lecture Notes in Artificial Intelligence, vol. LNAI 4648. Berlin, Germany: Springer-Verlag, 2007, pp. 555–564.
- [21] A. L. Christensen, R. O’Grady, and M. Dorigo, “Synchronization and fault detection in autonomous robots,” in *Proceedings of the 2008 IEEE/RSJ International Conference on Intelligent Robots and Systems (IROS-2008)*, R. Chatila, J. P. Merlet, and C. Laugier, Eds. Los Alamitos, CA: IEEE Computer Society Press, 2008, pp. 4139–4140.
- [22] S. Nouyan, R. Groß, M. Bonani, F. Mondada, and M. Dorigo, “Teamwork in self-organized robot colonies,” *IEEE Transactions on Evolutionary Computation*, vol. 13, no. 4, 2009, pp. 695–711.
- [23] A. G. Millard, J. Timmis, and A. F. T. Winfield, “Towards Exogenous Fault Detection in Swarm Robotic Systems,” 2014, pp. 429–430.
- [24] J. D. Bjerknes and A. F. T. Winfield, “On Fault Tolerance and Scalability of Swarm Robotic Systems,” in *Springer Tracts in Advanced Robotics*, 2013, vol. 83 STAR, pp. 431–444.
- [25] F. Higgins, A. Tomlinson, and K. M. Martin, “Survey on Security Challenges for Swarm Robotics,” in *2009 Fifth International Conference on Autonomic and Autonomous Systems*. IEEE, 2009, pp. 307–312.
- [26] A. F. Winfield and J. Nembrini, “Safety in numbers: fault-tolerance in robot swarms,” *International Journal of Modelling, Identification and Control*, vol. 1, no. 1, 2006, p. 30.
- [27] I. Sargeant and A. Tomlinson, “Review of Potential Attacks on Robotic Swarms,” in *Proceedings of SAI Intelligent Systems Conference (IntelliSys) 2016*, ser. Lecture Notes in Networks and Systems, Y. Bi, S. Kapoor, and R. Bhatia, Eds., vol. 15. Cham: Springer International Publishing, 2016, pp. 628–646.
- [28] V. Strobel, E. Castelló Ferrer, and M. Dorigo, “Managing byzantine robots via blockchain technology in a swarm robotics collective decision making scenario,” in *Proceedings of the 17th International Conference on Autonomous Agents and MultiAgent Systems*, ser. AAMAS ’18. Richland, SC: International Foundation for Autonomous Agents and Multiagent Systems, 2018, pp. 541–549.
- [29] M. Dorigo et al., “Swarmanoid: A novel concept for the study of heterogeneous robotic swarms,” *IEEE Robotics Automation Magazine*, vol. 20, no. 4, Dec 2013, pp. 60–71.
- [30] J. Werfel, K. Petersen, and R. Nagpal, “Designing collective behavior in a termite-inspired robot construction team,” *Science*, vol. 343, no. 6172, 2014, pp. 754–758.
- [31] R. C. Merkle, “A Digital Signature Based on a Conventional Encryption Function,” 1988, pp. 369–378.
- [32] F. Li, M. Hadjieleftheriou, G. Kollios, and L. Reyzin, “Dynamic authenticated index structures for outsourced databases,” in *Proceedings of the 2006 ACM SIGMOD International Conference on Management of Data*, ser. SIGMOD ’06. New York, NY, USA: ACM, 2006, pp. 121–132.

- [33] D. Hintze and A. Rice, "Picky: Efficient and reproducible sharing of large datasets using merkle-trees," *Proceedings - 2016 IEEE 24th International Symposium on Modeling, Analysis and Simulation of Computer and Telecommunication Systems, MASCOTS 2016*, 2016, pp. 30–38.
- [34] M. S. Niaz and G. Saake, "Merkle hash tree based techniques for data integrity of outsourced data," *CEUR Workshop Proceedings*, vol. 1366, 2015, pp. 66–71.
- [35] W. Du, R. Wang, and P. Ning, "An efficient scheme for authenticating public keys in sensor networks," in *Proceedings of the 6th ACM International Symposium on Mobile Ad Hoc Networking and Computing*, ser. *MobiHoc '05*. New York, NY, USA: ACM, 2005, pp. 58–67.
- [36] L. Zhou and C. Ravishankar, "Dynamic Merkle Trees for Verifying Privileges in Sensor Networks," in *2006 IEEE International Conference on Communications*, vol. 5, no. c. IEEE, 2006, pp. 2276–2282.
- [37] H. Halpin, "Updatechain: Using Merkle Trees for Software Updates," 2016, pp. 1–15.
- [38] B. P. Gerkey and M. J. Mataric, "A Formal Analysis and Taxonomy of Task Allocation in Multi-Robot Systems," *The International Journal of Robotics Research*, vol. 23, no. 9, sep 2004, pp. 939–954.
- [39] C. Pinciroli et al., "ARGoS: a modular, parallel, multi-engine simulator for multi-robot systems," *Swarm Intelligence*, vol. 6, no. 4, dec 2012, pp. 271–295.
- [40] L. Garattoni and M. Birattari, "Autonomous task sequencing in a robot swarm," *Science Robotics*, vol. 3, no. 20, jul 2018.
- [41] C. E. Shannon, "A mathematical theory of communication," *Bell System Technical Journal*, vol. 27, no. 3, 1948, pp. 379–423.
- [42] S. Halevi, D. Harnik, B. Pinkas, and A. Shulman-Peleg, "Proofs of ownership in remote storage systems," in *Proceedings of the 18th ACM Conference on Computer and Communications Security*, ser. *CCS '11*. New York, NY, USA: ACM, 2011, pp. 491–500.